Spatial Modulation Aided Layered Division Multiplexing: A Spectral Efficiency Perspective

Yue Sun, *Student Member, IEEE*, Jintao Wang, *Senior Member, IEEE*, Changyong Pan, *Senior Member, IEEE*, Longzhuang He, *Student Member, IEEE*, and Bo Ai, *Senior Member, IEEE*

Abstract—In this paper, spatial modulation (SM) is introduced to layered division multiplexing (LDM) systems for enlarging the spectral efficiency (SE) over broadcasting transmission. First, the SM aided LDM (SM-LDM) system is proposed, in which different layered services utilize SM for terrestrial broadcasting transmission with different power levels. Then a SE analysis framework for SM-LDM systems is proposed, which is suitable for the SM-LDM systems with linear combining. Moreover, the closed-form SE lower bound of SM-LDM systems with maximum ratio combining (MRC) is derived, which is based on this framework. Since the theoretical SE analysis of single transmit antenna (TA) LDM systems with MRC and spatial multiplexing (SMX) aided LDM systems with MRC lacks a closed-form expression, the closed-form SE is also derived for these systems. Monte Carlo simulations are provided to verify the tightness of our proposed SE lower bound. Furthermore, it can be shown via simulations that our proposed SM-LDM systems always have a better SE performance than single-TA LDM systems, which can even outperform the SE of SMX aided LDM (SMX-LDM) systems.

Index Terms—Layered division multiplexing (LDM); Spatial modulation (SM); terrestrial broadcasting transmission; spectral efficiency (SE).

I. INTRODUCTION

LAYERED division multiplexing (LDM) technology is recently proposed to satisfy the rapidly increasing spectral efficiency (SE) demand of digital terrestrial television (DTT) transmission, which has been accepted in the Advanced Television Systems Committee (ATSC) 3.0 standard [1]–[6]. As a non-orthogonal multiplexing technology, LDM simultaneously transmits different layered services at different power levels. Comparing with traditional time division multiplexing (TDM) and frequency division multiplexing (FDM), LDM has a higher SE, which is benefited from power allocation of different services [5]. Since different layers share the main part of physical layer modules, the LDM system only has a slightly higher complexity than the FDM or TDM system [3].

For LDM systems, in most instances there are two layers, i.e., the upper layer (UL) and the lower layer (LL), and the UL is allocated with a higher power level than the LL [4]. The UL

delivers low data rate service for mobile receivers, and the LL delivers high data rate service for fixed receivers. Therefore, the UL and the LL are also referred to as mobile layer (ML) and fixed layer (FL), respectively. When detecting the ML service, the FL service is treated as additional interference, and when detecting the FL service, the ML service need to be cancelled first [6].

Spatial modulation (SM) is proposed as a novel architecture of multiple-input multiple-output (MIMO) systems, which only activates one transmit antenna (TA) for delivering the constellation symbol in each time slot with only one radio frequency (RF) chain [7] [8]. Therefore, the information can be transmitted from both the spatial domain and constellation domain, and SM systems can achieve a better energy efficiency (EE) than traditional MIMO systems. In addition, with only one TA active in each time slot, SM has a more relaxed inter-antenna-synchronization (IAS) than traditional MIMO systems, and SM has no inter-channel interference (ICI) [8].

In broadcasting transmission scenarios, the cross-polarized 2×2 MIMO has been adopted in many standards, such as the Digital Video Broadcasting-Next Generation Handheld (DVB-NGH) [9], ATSC 3.0 [10] and the extension of the Integrated Services Digital Broadcasting-Terrestrial (ISDB-T) [11]. For next generation broadcasting system, the MIMO with more than 2 TAs has also been researched [12]–[14], and the MIMO precoding schemes are also introduced [14] [15]. Even massive MIMO is investigated in terrestrial broadcasting systems [16]. SM systems are also introduced to obtain a better trade-off of SE and EE for broadcasting transmission [17] [18]. More specifically, in [17], SM is combined with massive MIMO and orthogonal frequency division multiplexing (OFDM) in high speed train systems, and in [18], a block-sparse compressive sensing (BS-CS) based method is proposed for detection of GenSM with NOMA in terrestrial return channel.

For LDM technology, traditional MIMO scheme, including Alamouti coding and spatial multiplexing (SMX), has been adopted to improve system performance [5], and LDM combining with the multi-RF channel technology time frequency slicing (TFS) is also analyzed [19]. Since SM and LDM both need less RF chains, and SM can improve the SE by transmitting additional information via spatial domain, it is of great significant to investigate the SM combining with LDM. However, to the best of our knowledge, there are no research about the SM system combined with LDM system. Therefore, in this paper, we combine the SM system with a two-layer LDM system, which is denoted as the SM aided LDM (SM-LDM) system. In this SM-LDM system, both

the ML service and FL service utilize SM for terrestrial broadcasting transmission. The SE analysis framework of SM-LDM systems with linear combining is also proposed, and the closed-form SE lower bound of SM-LDM systems with maximum ratio combining (MRC) is derived by calculating out the signal-to-interference-plus-noise-ratio (SINR) value. We show simulation results that the SM-LDM system can achieve a quite efficient SE gain with not so low SNR. In addition, since the derived SE of single-TA LDM systems with MRC and SMX aided LDM (SMX-LDM) systems with MRC lack the closed-form expressions [4] [5], we also derive the closed-form SE of these systems.[1]

The organization of this paper is summarized as follows. In Section II, the system model of our proposed SM-LDM is introduced. In Section III, the SE analysis framework of SM-LDM systems with linear combining is proposed. In Section IV, the closed-form SE lower bound of SM-LDM systems with MRC is derived by calculating out the SINR. Section V presents the Monte Carlo simulation results to show the tightness of our proposed SE lower bound of SM-LDM systems with MRC, and the comparison between SM-LDM systems and other LDM schemes are also provided in this section. Finally, Section VI concludes this paper.

Notations: In this paper, the uppercase and lowercase bold-face letters represent matrices and column vectors, respectively. The operators $|\cdot|$, $(\cdot)^T$, $(\cdot)^H$ and $\|(\cdot)\|$ indicate the absolute function, transposition, conjugate transposition and Frobenius norm, respectively. The abbreviations $\det(\mathbf{A})$ and $\mathbf{A}(i,j)$ denote the determinant of matrix $\mathbf{A}$ and the component of $\mathbf{A}$ in i-th row and j-th column, respectively. The abbreviation $\mathrm{diag}(\mathbf{x})$ represents a diagonal matrix with diagonal elements $\mathbf{x}$. $\mathcal{P}(\cdot)$ denotes the probability density function, $\mathcal{CN}(\boldsymbol{\mu}, \boldsymbol{\Sigma})$ denotes a circularly symmetric multi-variate complex Gaussian distribution with mean $\boldsymbol{\mu}$ and covariance $\boldsymbol{\Sigma}$, and $\mathcal{CN}(\mathbf{x}; \boldsymbol{\mu}, \boldsymbol{\Sigma})$ denotes the probability density function (PDF) of the random vector $\mathbf{x} \sim \mathcal{CN}(\boldsymbol{\mu}, \boldsymbol{\Sigma})$. Besides, the abbreviation $E_{\mathbf{h}}\{\cdot\}$ represents taking expectations over random realizations of the vector $\mathbf{h}$.

II. SYSTEM MODEL

In this paper, a two-layer SM-LDM downlink model for terrestrial broadcasting transmission is introduced, which can also be easily extended to a multi-layer SM-LDM downlink model. As shown in Fig. 1 (a), at the transmitter, first the SM transmitting symbols of ML and FL are separately generated in frequency domain. Therefore, after the ML SM mapper and FL SM mapper, the ML and FL SM symbols in frequency domain, i.e., $\mathbf{x}_{\mathrm{ml}} \in \mathbb{C}^{N_t \times 1}$ and $\mathbf{x}_{\mathrm{fl}} \in \mathbb{C}^{N_t \times 1}$, can be denoted as follows:

$$\mathbf{x}_{\mathrm{ml}} = s_{\mathrm{ml}}\mathbf{a}_{\mathrm{ml}}, \quad \mathbf{x}_{\mathrm{fl}} = s_{\mathrm{fl}}\mathbf{a}_{\mathrm{fl}}, \tag{1}$$

where N_{t} represents the number of TAs, and s_{ml} and s_{fl} denote the constellation symbols of ML and FL, respectively.

[1]In broadcasting system, since the transmission power is relatively high, it is difficult to split power to feed different TAs. However, the specific hardware implementation is not involved in this paper, so this effect is beyond the scope of this paper. Besides, some MIMO precoders are also investigated in next generation broadcasting system, which also involve the power allocation between different TAs [14] [15].
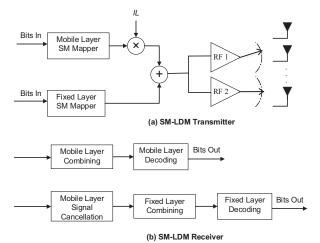

(a) **SM-LDM Transmitter**

(b) **SM-LDM Receiver**

Fig. 1. Transmitter and receiver for the two-layer SM-LDM system.

Besides, $\mathbf{a}_{\mathrm{ml}} = [0, \ldots, 0, 1, 0, \ldots, 0]^T \in \mathbb{C}^{N_t \times 1}$ and $\mathbf{a}_{\mathrm{fl}} = [0, \ldots, 0, 1, 0, \ldots, 0]^T \in \mathbb{C}^{N_t \times 1}$ denote the active antenna of ML and FL, respectively. Aided by SM property, only one element of $\mathbf{a}_{\mathrm{ml}}$ or $\mathbf{a}_{\mathrm{fl}}$ is equal to 1, which represents the active antenna.

Then the injection level, *IL*, is introduced to control the power allocation between the two layers [5]. For SM-OFDM scheme, each subcarrier relies on one TA [17], so each constellation symbol in frequency domain is allocated with one active antenna. After that, since each layer needs one RF chain for transmitting the SM symbol, for the two-layer SM-LDM transmitter only two RF chains are enough. Therefore, in our proposed two-layer SM-LDM system, the transmitted symbol in frequency domain can be denoted as follows:

$$\mathbf{x} = \sqrt{\rho_{\mathrm{ml}}}\mathbf{x}_{\mathrm{ml}} + \sqrt{\rho_{\mathrm{fl}}}\mathbf{x}_{\mathrm{fl}}, \tag{2}$$

where ρ_{ml} and ρ_{fl} denote the transmit power of ML and FL, respectively. Since the ML is allocated with a higher power than FL, we have:

$$\rho_{\mathrm{ml}} + \rho_{\mathrm{fl}} = P_{\mathrm{u}}, \quad \rho_{\mathrm{ml}}/\rho_{\mathrm{fl}} = IL, \quad IL > 0 \text{ dB}, \tag{3}$$

where P_{u} denotes the total transmit power.

At the mobile receiver, as shown in Fig. 1 (b), the FL symbol is regarded as additional interference, and we denote N_{rm} as the number of receive antennas (RAs) in ML. Thus the received symbol can be denoted as follows:

$$\mathbf{y}_{\mathrm{ml}} = \mathbf{H}_{\mathrm{ml}} \left(\sqrt{\rho_{\mathrm{ml}}}\mathbf{x}_{\mathrm{ml}} + \sqrt{\rho_{\mathrm{fl}}}\mathbf{x}_{\mathrm{fl}}\right) + \mathbf{n}_{\mathrm{ml}}, \tag{4}$$

where $\mathbf{H}_{\mathrm{ml}} \in \mathbb{C}^{N_{\mathrm{rm}} \times N_t}$ represents the frequency-domain channel matrix between the transmitter and the ML receiver. Assuming a Wide Sense Stationary (WSS) Rayleigh fading channel [4], each element of $\mathbf{H}_{\mathrm{ml}}$ is an independent and identically distributed (i.i.d.) Gaussian random variable with mean 0 and variance 1. In addition, $\mathbf{n}_{\mathrm{ml}} \in \mathbb{C}^{N_{\mathrm{rm}} \times 1}$ denotes the additive white Gaussian noise (AWGN) of ML with $\mathbf{n}_{\mathrm{ml}} \sim \mathcal{CN}(\mathbf{0}, \sigma_{\mathrm{ml}}^2\mathbf{I})$, and σ_{ml}^2 is the noise variance of ML.

At the fixed receiver, N_{rf} denotes the number of RAs, and the received symbol can be denoted as follows:

$$\mathbf{y}_{\mathrm{fl}} = \mathbf{H}_{\mathrm{fl}} \left(\sqrt{\rho_{\mathrm{ml}}}\mathbf{x}_{\mathrm{ml}} + \sqrt{\rho_{\mathrm{fl}}}\mathbf{x}_{\mathrm{fl}}\right) + \mathbf{n}_{\mathrm{fl}}, \tag{5}$$

where $\mathbf{H}_{\mathrm{fl}} \in \mathbb{C}^{N_{\mathrm{rf}} \times N_{\mathrm{t}}}$ is the channel matrix between the transmitter and the FL receiver in frequency domain, which can also be assumed as a WSS Rayleigh fading channel, so each element of $\mathbf{H}_{\mathrm{fl}}$ is i.i.d. Gaussian random variable with $\mathbf{H}_{\mathrm{fl}}(i,j) \sim \mathcal{CN}(0,1)$. $\mathbf{n}_{\mathrm{fl}} \in \mathbb{C}^{N_{\mathrm{rf}} \times 1}$ is the AWGN of FL with $\mathbf{n}_{\mathrm{fl}} \sim \mathcal{CN}(\mathbf{0}, \sigma_{\mathrm{fl}}^2 \mathbf{I})$, and σ_{fl}^2 is the noise variance of FL. The ML noise always has a higher power level than the FL noise, and thus we have $\sigma_{\mathrm{ml}}^2 > \sigma_{\mathrm{fl}}^2$.

When detecting the symbols of FL, as shown in Fig. 1 (b), before detecting the FL signal, the ML signal is cancelled first. In the typical ATSC 3.0 scenarios, the FL always has a much higher signal-to-noise-ratio (SNR) than that of ML [4], so we assume the perfect ML signal cancellation. However, after the perfect ML signal cancellation, the cross-layer interference (CLI) still might be introduced because of the non-ideal channel estimation (CE). Fortunately, since a properly designed CE module can provide a CE mean square error (MSE) lower than -30 dB [6], the CLI is not explicitly considered [5]. Therefore, after the ML signal cancellation, the received symbol of FL can be denoted as follows:

$$\mathbf{y}_{\mathrm{fl}} = \sqrt{\rho_{\mathrm{fl}}}\mathbf{H}_{\mathrm{fl}}\mathbf{x}_{\mathrm{fl}} + \mathbf{n}_{\mathrm{fl}}, \tag{6}$$

and the following SE analysis of FL is also based on (6).

It should be noted that, for both $\mathbf{H}_{\mathrm{ml}}$ and $\mathbf{H}_{\mathrm{fl}}$, the TA correlation is not considered. This assumption is the same as that in [5], and [5] investigates the channel capacity of LDM over MIMO transmission. This is because there are only 2 or 4 TAs in this two-layer SM-LDM system, and the half-wave antenna spacing is assumed for a moment. This assumption is not entirely practical, and the TA correlation will be considered in future work.

III. SE ANALYSIS FRAMEWORK

In this section, the SE analysis framework for SM-LDM systems with linear combining is separately proposed for ML and FL. Besides, the SE analysis frameworks for single-TA LDM systems and SMX-LDM systems are also proposed. In our proposed SE analysis frameworks, the SINR determined by specific combining schemes is the only variable. By substituting the derived SINR into the SE analysis framework, the closed-form SE can be formulated. Moreover, our proposed SE analysis framework can be easily extended to the multi-layer SM-LDM systems.

A. Analysis for ML

The received symbol of ML in (4) can be transformed as a vector form, which is denoted as follows:

$$\begin{aligned} \mathbf{y}_{\mathrm{ml}} = &\sum_{n=1}^{N_{\mathrm{t}}} \sqrt{\rho_{\mathrm{ml}}} s_{\mathrm{ml},n} \gamma_{\mathrm{ml},n} \mathbf{h}_{\mathrm{ml},n} \\ &+ \sum_{m=1}^{N_{\mathrm{t}}} \sqrt{\rho_{\mathrm{fl}}} s_{\mathrm{fl},m} \gamma_{\mathrm{fl},m} \mathbf{h}_{\mathrm{ml},m} + \mathbf{n}_{\mathrm{ml}}, \end{aligned} \tag{10}$$

where $s_{\mathrm{ml},n} \sim \mathcal{CN}(0,1)$ and $s_{\mathrm{fl},m} \sim \mathcal{CN}(0,1)$ denote the Gaussian inputs of ML and FL, respectively. $\gamma_{\mathrm{ml},n}$ and $\gamma_{\mathrm{fl},m}$ represent the activity of the n-th TA for ML and m-th TA for FL, respectively. Aided by SM property, $\sum_{n=1}^{N_{\mathrm{t}}} \gamma_{\mathrm{ml},n} =$

$\sum_{m=1}^{N_{\mathrm{t}}} \gamma_{\mathrm{fl},m} = 1$, $\mathcal{P}(\gamma_{\mathrm{ml},n} = 1) = \mathcal{P}(\gamma_{\mathrm{fl},m} = 1) = \frac{1}{N_{\mathrm{t}}}$ and $\mathcal{P}(\gamma_{\mathrm{ml},n} = 0) = \mathcal{P}(\gamma_{\mathrm{fl},m} = 0) = \frac{N_{\mathrm{t}}-1}{N_{\mathrm{t}}}$. In addition, $\mathbf{h}_{\mathrm{ml},n} \in \mathbb{C}^{N_{\mathrm{rm}} \times 1}$ denotes the n-th column of $\mathbf{H}_{\mathrm{ml}}$.

With linear combining, $\mathbf{g}_{\mathrm{ml},n}$ is denoted as the combining vector for the n-th TA in ML. Therefore, the SINR corresponding to the n-th TA of ML, i.e., $\mathrm{SINR}_{\mathrm{ml},n}$ can be lower bounded as (7), which can be proved from a direct application of [20, Lemma 1]. In (7), the numerator denotes the received power of the needed n-th transmit symbol in ML. The first two terms of the denominator in (7) represent the received power of other transmit symbols in ML, i.e., the inter-antenna-interference (IAI) introduced by ML. The third term of the denominator in (7) denotes the received power of transmit symbols in FL, which can be regarded as the interference introduced by FL. The forth term of the denominator in (7) represents the influence of AWGN.

Aided by the SINR expression in (7), an additive noise approximation can be introduced to (10), and (10) can be transformed as follows:

$$\hat{\mathbf{y}}_{\mathrm{ml}} = \mathbf{x}_{\mathrm{ml}} + \mathbf{w}_{\mathrm{ml}}, \tag{11}$$

where $\hat{\mathbf{y}}_{\mathrm{ml}} \in \mathbb{C}^{N_{\mathrm{t}} \times 1}$ represents the equivalent received symbol in ML, and $\mathbf{w}_{\mathrm{ml}} \in \mathbb{C}^{N_{\mathrm{t}} \times 1}$ is a circularly symmetric complex-valued Gaussian noise, whose mean is $\mathbf{0}$ and the covariance matrix is denoted as follows:

$$E\left\{\mathbf{w}_{\mathrm{ml}}\mathbf{w}_{\mathrm{ml}}^H\right\} = \mathrm{diag}\left\{\frac{1}{\mathrm{SINR}_{\mathrm{ml},1}}, \cdots, \frac{1}{\mathrm{SINR}_{\mathrm{ml},N_{\mathrm{t}}}}\right\}. \tag{12}$$

Thus the mutual information (MI) can be divided into the spatial-domain MI and constellation-domain MI, which can be denoted as follows:

$$I(\hat{\mathbf{y}}_{\mathrm{ml}}; \mathbf{x}_{\mathrm{ml}}) = I(\hat{\mathbf{y}}_{\mathrm{ml}}; \mathbf{a}_{\mathrm{ml}}) + I(\hat{\mathbf{y}}_{\mathrm{ml}}; \mathbf{x}_{\mathrm{ml}}|\mathbf{a}_{\mathrm{ml}}). \tag{13}$$

Then aided by SM principle, in SM-LDM systems, the SE of ML with linear combining can be derived, and Theorem 1 is introduced.

Theorem 1: The downlink SE of ML in SM-LDM systems with linear combining can be lower bounded as (9), where $\boldsymbol{\Sigma}_{\mathrm{ml},n}$ can be denoted as follows:

$$\boldsymbol{\Sigma}_{\mathrm{ml},n} = \mathrm{diag}\left\{\frac{1}{\mathrm{SINR}_{\mathrm{ml},1}}, ..., \frac{1}{\mathrm{SINR}_{\mathrm{ml},N_{\mathrm{t}}}}\right\} + N_{\mathrm{t}}\mathrm{diag}\{\hat{\mathbf{a}}_{\mathrm{ml},n}\}, \tag{14}$$

and $\hat{\mathbf{a}}_{\mathrm{ml},n}$ represents the n-th column of an N_{t}-by-N_{t} identity matrix $\mathbf{I}_{N_{\mathrm{t}}}$.

Proof: When the active antenna of ML is determined, the constellation-domain MI in (13) can be quantified by Shannon's continuous-input continuous-output channel (CM-CC) capacity [21], and thus we have:

$$I(\hat{\mathbf{y}}_{\mathrm{ml}}; \mathbf{x}_{\mathrm{ml}}|\mathbf{a}_{\mathrm{ml}}) = \frac{1}{N_{\mathrm{t}}}\sum_{n=1}^{N_{\mathrm{t}}} \log_2(1 + N_{\mathrm{t}}\mathrm{SINR}_{\mathrm{ml},n}). \tag{15}$$

$$\text{SINR}_{\text{ml},n} = \frac{\frac{\rho_{\text{ml}}}{N_{\text{t}}} \left| E_{\mathbf{h}} \left\{ \mathbf{g}_{\text{ml},n}^H \mathbf{h}_{\text{ml},n} \right\} \right|^2}{\sum_{n'=1}^{N_{\text{t}}} \frac{\rho_{\text{ml}}}{N_{\text{t}}} E_{\mathbf{h}} \left\{ \left| \mathbf{g}_{\text{ml},n}^H \mathbf{h}_{\text{ml},n'} \right|^2 \right\} - \frac{\rho_{\text{ml}}}{N_{\text{t}}} \left| E_{\mathbf{h}} \left\{ \mathbf{g}_{\text{ml},n}^H \mathbf{h}_{\text{ml},n} \right\} \right|^2 + \sum_{m=1}^{N_{\text{t}}} \frac{\rho_{\text{fl}}}{N_{\text{t}}} E_{\mathbf{h}} \left\{ \left| \mathbf{g}_{\text{ml},n}^H \mathbf{h}_{\text{ml},m} \right|^2 \right\} + \sigma_{\text{ml}}^2 E_{\mathbf{h}} \left\{ \| \mathbf{g}_{\text{ml},n} \|^2 \right\}}, \quad (7)$$

$$I\left(\hat{\mathbf{y}}_{\text{ml}}; \mathbf{x}_{\text{ml}}\right) = \frac{1}{N_{\text{t}}} \left\{ \sum_{n=1}^{N_{\text{t}}} \log_2 \left(1 + N_{\text{t}} \text{SINR}_{\text{ml},n}\right) + \sum_{n=1}^{N_{\text{t}}} E_{\mathbf{y} \sim \mathcal{CN}(\mathbf{0}, \boldsymbol{\Sigma}_{\text{ml},n})} \left[\log_2 \left(\frac{\mathcal{P}(\mathbf{y}|\hat{\mathbf{a}}_{\text{ml},n})}{\frac{1}{N_{\text{t}}} \sum_{n'=1}^{N_{\text{t}}} \mathcal{P}(\mathbf{y}|\hat{\mathbf{a}}_{\text{ml},n'})} \right) \right] \right\}, \quad (8)$$

$$I^{\text{lb}}\left(\hat{\mathbf{y}}_{\text{ml}}; \mathbf{x}_{\text{ml}}\right) = \log_2(N_{\text{t}}) - N_{\text{t}} + \frac{1}{N_{\text{t}}} \left\{ \sum_{n=1}^{N_{\text{t}}} \log_2 \left(1 + N_{\text{t}} \text{SINR}_{\text{ml},n}\right) - \sum_{n=1}^{N_{\text{t}}} \log_2 \left[\sum_{n'=1}^{N_{\text{t}}} \frac{\det\left(\boldsymbol{\Sigma}_{\text{ml},n}\right)}{\det\left(\boldsymbol{\Sigma}_{\text{ml},n} + \boldsymbol{\Sigma}_{\text{ml},n'}\right)} \right] \right\}, \quad (9)$$

According to the definition of MI in (8), the spatial-domain MI term in (13) can be denoted as follows:

$$I(\hat{\mathbf{y}}_{\text{ml}}; \mathbf{a}_{\text{ml}}) = \text{T}_1 - \text{T}_2$$

$$= \frac{1}{N_{\text{t}}} \int \sum_{n=1}^{N_{\text{t}}} \mathcal{P}(\hat{\mathbf{y}}_{\text{ml}}|\hat{\mathbf{a}}_{\text{ml},n}) \log_2 \mathcal{P}(\hat{\mathbf{y}}_{\text{ml}}|\hat{\mathbf{a}}_{\text{ml},n}) d\hat{\mathbf{y}}_{\text{ml}} -$$

$$\frac{1}{N_{\text{t}}} \int \sum_{n=1}^{N_{\text{t}}} \mathcal{P}(\hat{\mathbf{y}}_{\text{ml}}|\hat{\mathbf{a}}_{\text{ml},n}) \log_2 \left[\frac{1}{N_{\text{t}}} \sum_{n'=1}^{N_{\text{t}}} \mathcal{P}(\hat{\mathbf{y}}_{\text{ml}}|\hat{\mathbf{a}}_{\text{ml},n'}) \right] d\hat{\mathbf{y}}_{\text{ml}}, \quad (16)$$

where $\mathcal{P}(\hat{\mathbf{y}}_{\text{ml}}|\hat{\mathbf{a}}_{\text{ml},n}) = \mathcal{CN}(\hat{\mathbf{y}}_{\text{ml}}; \mathbf{0}, \boldsymbol{\Sigma}_{\text{ml},n})$ is a likelihood function.

In (16), the term T_1 can be directly calculated out as follows:

$$\text{T}_1 = -N_{\text{t}} \log_2(\pi e) - \frac{1}{N_{\text{t}}} \sum_{n=1}^{N_{\text{t}}} \log_2(\det(\boldsymbol{\Sigma}_{\text{ml},n})). \quad (17)$$

However, the term T_2 lacks a closed-form solution, so the Jensen's inequality is introduced for approximation as follows:

$$\text{T}_2 \leq$$

$$\frac{1}{N_{\text{t}}} \sum_{n=1}^{N_{\text{t}}} \log_2 \left[\frac{1}{N_{\text{t}}} \sum_{n'=1}^{N_{\text{t}}} \int \mathcal{P}(\hat{\mathbf{y}}_{\text{ml}}|\hat{\mathbf{a}}_{\text{ml},n}) \mathcal{P}(\hat{\mathbf{y}}_{\text{ml}}|\hat{\mathbf{a}}_{\text{ml},n'}) d\hat{\mathbf{y}}_{\text{ml}} \right]$$

$$= \frac{1}{N_{\text{t}}} \sum_{n=1}^{N_{\text{t}}} \log_2 \left[\sum_{n'=1}^{N_{\text{t}}} \frac{\frac{1}{N_{\text{t}}}}{\det(\boldsymbol{\Sigma}_{\text{ml},n} + \boldsymbol{\Sigma}_{\text{ml},n'})} \right] - N_{\text{t}} \log_2 \pi. \quad (18)$$

By substituting (17) and (18) into (16), the spatial-domain MI term can be lower bounded as follows:

$$I(\hat{\mathbf{y}}_{\text{ml}}; \mathbf{a}_{\text{ml}}) \geq \log_2 N_{\text{t}}$$

$$- \frac{1}{N_{\text{t}}} \sum_{n=1}^{N_{\text{t}}} \log_2 \left[\sum_{n'=1}^{N_{\text{t}}} \frac{\det(\boldsymbol{\Sigma}_{\text{ml},n})}{\det(\boldsymbol{\Sigma}_{\text{ml},n} + \boldsymbol{\Sigma}_{\text{ml},n'})} \right] - N_{\text{t}} \log_2 e. \quad (19)$$

Moreover, aided by SM principle, when all SINRs of ML approximate to infinity, the spatial-domain MI of ML should approximate to $\log_2 N_{\text{t}}$. Besides, when all SINRs of ML approximate to 0, the spatial-domain MI of ML should approximate to 0. However, the limitations of derived lower bound in (19) are different, and each limitation lacks a constant bias. To achieve an unbiased SE lower bound, a constant shift is applied in (19), and the asymptotically unbiased spatial-domain MI lower bound can be derived as follows:

$$I(\hat{\mathbf{y}}_{\text{ml}}; \mathbf{a}_{\text{ml}}) \succeq \log_2(N_{\text{t}}) - N_{\text{t}}$$

$$- \frac{1}{N_{\text{t}}} \sum_{n=1}^{N_{\text{t}}} \log_2 \left[\sum_{n'=1}^{N_{\text{t}}} \frac{\det(\boldsymbol{\Sigma}_{\text{ml},n})}{\det(\boldsymbol{\Sigma}_{\text{ml},n} + \boldsymbol{\Sigma}_{\text{ml},n'})} \right]. \quad (20)$$

Therefore, by substituting (15) and (20) into (13), the SE lower bound of ML can be formulated as (9), which completes this proof. ∎

Therefore, with a specific linear combining algorithm, the closed-form SINR in (7) can be derived, and then aided by Theorem 1, the theoretical value of ML SE in (9) can be formulated.

From the proof of Theorem 1, it can be shown that the gap between the theoretical SE and SE lower bound comes from the approximation of spatial-domain MI. More specifically, the Jensen's inequality is applied in (18) for deriving the closed-form lower bound of T_2, i.e., the second term of spatial-domain MI. Since the approximation of Jensen's inequality introduces the MI loss, a constant shift is applied to ensure an unbiased lower bound of spatial-domain MI in (20).

B. Analysis for FL

Aided by (6), the received symbol of FL can also be transformed as a vector form as follows:

$$\mathbf{y}_{\text{fl}} = \sum_{m=1}^{N_{\text{t}}} \sqrt{\rho_{\text{fl}}} s_{\text{fl},m} \gamma_{\text{fl},m} \mathbf{h}_{\text{fl},m} + \mathbf{n}_{\text{fl}}. \quad (21)$$

For FL, $\mathbf{g}_{\text{fl},m}$ represents the linear combining vector for the m-th TA, and the SINR of the m-th TA can be lowered bounded as (22). From (22), it can be seen that the numerator represents the received power of the transmit symbol of the m-th TA in FL, the first two terms of the denominator denote the IAI introduced by FL, and the last term of the denominator denotes the influence of AWGN. Different from the SINR of ML in (7), for SINR of FL, only the transmit symbols of FL introduce the IAI, and the transmit symbols of ML have no influence on the SINR of FL assuming perfect cancellation.

Aided by the ML SE analysis in the proof of Theorem 1, the downlink FL SE can be lower bounded as (23), where $\boldsymbol{\Sigma}_{\text{fl},m}$ can be denoted as follows:

$$\boldsymbol{\Sigma}_{\text{fl},m} = \text{diag} \left\{ \frac{1}{\text{SINR}_{\text{fl},1}}, ..., \frac{1}{\text{SINR}_{\text{fl},N_{\text{t}}}} \right\} + N_{\text{t}} \text{diag}\{\hat{\mathbf{a}}_{\text{fl},m}\}, \quad (24)$$

and $\hat{\mathbf{a}}_{\text{fl},m}$ denotes the m-th column of $\mathbf{I}_{N_{\text{t}}}$.

From (9) and (23), it can be shown that SE lower bound expressions for both ML and FL are almost the same. However, the ML SE is influenced from both ML and FL transmit symbols, but the FL SE is only influenced by FL transmit symbols.

$$\text{SINR}_{\text{fl},m} = \frac{\frac{\rho_{\text{fl}}}{N_{\text{t}}} \left| E_{\mathbf{h}} \left\{ \mathbf{g}_{\text{fl},m}^H \mathbf{h}_{\text{fl},m} \right\} \right|^2}{\sum_{m'=1}^{N_{\text{t}}} \frac{\rho_{\text{fl}}}{N_{\text{t}}} E_{\mathbf{h}} \left\{ \left| \mathbf{g}_{\text{fl},m}^H \mathbf{h}_{\text{fl},m'} \right|^2 \right\} - \frac{\rho_{\text{fl}}}{N_{\text{t}}} \left| E_{\mathbf{h}} \left\{ \mathbf{g}_{\text{fl},m}^H \mathbf{h}_{\text{fl},m} \right\} \right|^2 + \sigma_{\text{fl}}^2 E_{\mathbf{h}} \left\{ \|\mathbf{g}_{\text{fl},m}\|^2 \right\}}, \tag{22}$$

$$I^{\text{lb}}(\hat{\mathbf{y}}_{\text{fl}}; \mathbf{x}_{\text{fl}}) = \log_2(N_{\text{t}}) - N_{\text{t}} + \frac{1}{N_{\text{t}}} \left\{ \sum_{m=1}^{N_{\text{t}}} \log_2(1 + N_{\text{t}} \text{SINR}_{\text{fl},m}) - \sum_{m=1}^{N_{\text{t}}} \log_2 \left[\sum_{m'=1}^{N_{\text{t}}} \frac{\det(\mathbf{\Sigma}_{\text{fl},m})}{\det(\mathbf{\Sigma}_{\text{fl},m} + \mathbf{\Sigma}_{\text{fl},m'})} \right] \right\}, \tag{23}$$

C. Analysis for Single-TA LDM and SMX-LDM

For conventional single-TA LDM systems, the SE of ML can be obtained by substituting $N_{\text{t}} = 1$ into (9), and the SE of FL can be obtained by substituting $N_{\text{t}} = 1$ into (23). Thus the SE of both ML and FL for single-TA LDM systems can be derived as follows:

$$R_{\text{ml}}^{\text{ST}} = \log_2(1 + \text{SINR}_{\text{ml}}^{\text{ST}}), \quad R_{\text{fl}}^{\text{ST}} = \log_2(1 + \text{SINR}_{\text{fl}}^{\text{ST}}), \tag{25}$$

where $R_{\text{ml}}^{\text{ST}}$ and $R_{\text{fl}}^{\text{ST}}$ represent the SE of ML and FL in single-TA LDM systems, respectively. In addition, $\text{SINR}_{\text{ml}}^{\text{ST}}$ and $\text{SINR}_{\text{fl}}^{\text{ST}}$ denote the SINR of ML and FL in single-TA LDM systems, respectively. The $\text{SINR}_{\text{ml}}^{\text{ST}}$ and $\text{SINR}_{\text{fl}}^{\text{ST}}$ can be obtained by substituting $N_{\text{t}} = 1$ into (7) and (22), respectively. In single-TA LDM systems, only the constellation symbols transmit information, so (25) represents the exact value of SE. The approximation is only conducted when deriving the spatial-domain MI.

For SMX-LDM systems, since all transmit antennas are active to transmit constellation symbols, the SE of ML and FL can be quantified by CMCC capacity as follows:

$$R_{\text{ml}}^{\text{SMX}} = \sum_{n=1}^{N_{\text{t}}} \log_2(1 + \text{SINR}_{\text{ml},n}^{\text{SMX}}),$$
$$R_{\text{fl}}^{\text{SMX}} = \sum_{m=1}^{N_{\text{t}}} \log_2(1 + \text{SINR}_{\text{fl},m}^{\text{SMX}}), \tag{26}$$

where $R_{\text{ml}}^{\text{SMX}}$ and $R_{\text{fl}}^{\text{SMX}}$ denote the SE of ML and FL in SMX-LDM systems, respectively. Besides, $\text{SINR}_{\text{ml},n}^{\text{SMX}}$ represents the SINR of the n-th TA in ML of SMX-LDM systems, and $\text{SINR}_{\text{fl},m}^{\text{SMX}}$ represents the SINR of the m-th TA in FL of SMX-LDM systems. Similarly, for SMX-LDM systems, (26) is the exact value rather than the lower bound, since only the constellation domain transmits information.

IV. CLOSED-FORM SE LOWER BOUND WITH MRC

In our proposed SE analysis framework, the SINR values are related to specific combining algorithms. In this section, MRC is considered for SM-LDM systems, single-TA LDM systems and SMX-LDM systems. In addition, the closed-form SE lower bound for SM-TDM/FDM systems with MRC is also formulated.

A. SM-LDM

In this subsection, MRC is considered for both ML and FL, and the SINR values of these two layers are derived as closed forms. Then substituting the closed-form SINR values into (9) and (23), the closed-form SE lower bound of SM-LDM systems with MRC can be formulated.

For MRC, the combining vector of the n-th TA for ML is the estimated n-th column of $\mathbf{H}_{\text{ml}}$, and the combining vector of the m-th TA for FL is the estimated m-th column of $\mathbf{H}_{\text{fl}}$. Since the perfect CE is assumed, we have:

$$\mathbf{g}_{\text{ml},n} = \mathbf{h}_{\text{ml},n}, \quad \mathbf{g}_{\text{fl},m} = \mathbf{h}_{\text{fl},m}. \tag{27}$$

Aided by (27), it can be immediately formulated as follows:

$$E_{\mathbf{h}} \left\{ \mathbf{g}_{\text{ml},n}^H \mathbf{h}_{\text{ml},n} \right\} = E_{\mathbf{h}} \left\{ \|\mathbf{g}_{\text{ml},n}\|^2 \right\} = N_{\text{rm}},$$
$$E_{\mathbf{h}} \left\{ \mathbf{g}_{\text{fl},m}^H \mathbf{h}_{\text{fl},m} \right\} = E_{\mathbf{h}} \left\{ \|\mathbf{g}_{\text{fl},m}\|^2 \right\} = N_{\text{rf}}. \tag{28}$$

For the interference terms in ML, if $n' \neq n$, $\mathbf{g}_{\text{ml},n}$ and $\mathbf{h}_{\text{ml},n'}$ are independent, and, thus we have:

$$E_{\mathbf{h}} \left\{ \left| \mathbf{g}_{\text{ml},n}^H \mathbf{h}_{\text{ml},n'} \right|^2 \right\} = E_{\mathbf{h}} \left\{ \|\mathbf{g}_{\text{ml},n}\|^2 \right\} = N_{\text{rm}}. \tag{29}$$

In addition, if $m = n$, $\mathbf{g}_{\text{ml},n}$ and $\mathbf{h}_{\text{ml},m}$ are correlated. In this case, aided by the property of the central complex-valued Wishart distribution [22], we have:

$$E_{\mathbf{h}} \left\{ \left| \mathbf{g}_{\text{ml},n}^H \mathbf{h}_{\text{ml},m} \right|^2 \right\} = E_{\mathbf{h}} \left\{ \|\mathbf{h}_{\text{ml},n}\|^4 \right\} = N_{\text{rm}}(N_{\text{rm}} + 1). \tag{30}$$

By substituting (28), (29) and (30) into (7), the SINR of the n-th TA in ML with MRC can be formulated as follows:

$$\text{SINR}_{\text{ml},n} = \frac{\rho_{\text{ml}} N_{\text{rm}}}{\rho_{\text{ml}} N_{\text{t}} + \rho_{\text{fl}}(N_{\text{t}} + N_{\text{rm}}) + N_{\text{t}} \sigma_{\text{ml}}^2}. \tag{31}$$

In (31), the numerator denotes the power of the targeted received symbol of ML, the first term of the denominator denotes the IAI caused by ML, the second term of the denominator denotes the interference introduced by FL, and the last term of the denominator represents the AWGN. In addition, from (31), it can be seen that increasing the number of RAs in ML or decreasing the number of TAs can bring a larger SINR for ML. Besides, although enlarging the transmit power of ML can also increase the SINR of ML, the SINR cannot increase indefinitely because of the interference caused by both ML and FL.

Following from a similar application of SINR derivation in ML, the SINR corresponding to the m-th TA of FL with MRC can be derived too, which can be denoted as follows:

$$\text{SINR}_{\text{fl},m} = \frac{\rho_{\text{fl}} N_{\text{rf}}}{\rho_{\text{fl}} N_{\text{t}} + N_{\text{t}} \sigma_{\text{fl}}^2}. \tag{32}$$

In (32), the numerator represents the power of the targeted received symbol in FL, the first term and the second term of the denominator represent the interference caused by FL and AWGN, respectively. Similarly, increasing the transmit power of FL can enlarge the SINR of FL. More RAs in FL or less TAs can also increase the SINR of FL.

Aided by the SINR of ML in (31), the closed-form SE lower bound for ML in SM-LDM systems with MRC can be derived

by substituting (31) into (7) and (9). The closed-form SE lower bound for FL in SM-LDM systems with MRC can also be derived by substituting (32) into (22) and (23).

B. Single-TA LDM and SMX-LDM

For single-TA LDM systems, the SINR of ML and FL can be derived by applying $N_{\mathrm{t}} = 1$ into (31) and (32), respectively. Thus we have:

$$
\begin{aligned}
\mathrm{SINR}_{\mathrm{ml}}^{\mathrm{ST}} &= \frac{\rho_{\mathrm{ml}} N_{\mathrm{rm}}}{\rho_{\mathrm{ml}} + \rho_{\mathrm{fl}}(1 + N_{\mathrm{rm}}) + \sigma_{\mathrm{ml}}^2}, \\
\mathrm{SINR}_{\mathrm{fl}}^{\mathrm{ST}} &= \frac{\rho_{\mathrm{fl}} N_{\mathrm{rf}}}{\rho_{\mathrm{fl}} + \sigma_{\mathrm{fl}}^2}.
\end{aligned}
\tag{33}
$$

By substituting (33) into (25), the SE exact value of single-TA LDM systems with MRC is derived. Comparing (33) with (31) and (32), the SINR of ML and FL in single-TA LDM systems is larger than the SINR of ML and FL for SM-LDM systems, respectively. This is because the IAI introduced by multiple TAs in SM-LDM system. From (15) and (25), it can be observed that a larger SINR leads to a larger constellation-domain MI, so the constellation-domain MI of single-TA LDM systems is larger than that of SM-LDM systems. However, the spatial domain can also be utilized for information transmission in SM-LDM systems, so the SE comparison between SM-LDM systems and single-TA LDM systems is conducted in the section of simulation results.

For SMX-LDM systems, to ensure the fairness of the same transmit power, comparing with SM-LDM systems, the transmit power of each TA should divide N_{t}. Thus we have:

$$
\begin{aligned}
\mathrm{SINR}_{\mathrm{ml},n}^{\mathrm{SMX}} &= \frac{\rho_{\mathrm{ml}} N_{\mathrm{rm}}}{\rho_{\mathrm{ml}} N_{\mathrm{t}} + \rho_{\mathrm{fl}}(N_{\mathrm{t}} + N_{\mathrm{rm}}) + N_{\mathrm{t}}^2 \sigma_{\mathrm{ml}}^2}, \\
\mathrm{SINR}_{\mathrm{fl},m}^{\mathrm{SMX}} &= \frac{\rho_{\mathrm{fl}} N_{\mathrm{rf}}}{\rho_{\mathrm{fl}} N_{\mathrm{t}} + N_{\mathrm{t}}^2 \sigma_{\mathrm{fl}}^2}.
\end{aligned}
\tag{34}
$$

By substituting (34) into (26), the SE exact value of SMX-LDM systems with MRC can also be formulated. From (34), (31) and (32), it can be seen that for SM-LDM systems and SMX-LDM systems, the interference terms of both ML and FL have a same influence on the SINR of ML and FL, respectively. However, the AWGN terms of both ML and FL in SMX-LDM systems are larger than those in SM-LDM systems, which is because the transmit power of each TA in SMX-LDM systems is smaller than that in SM-LDM systems.

C. SM-TDM/FDM

For SM-TDM/FDM systems, the ML services and FL services are transmitted separately in time domain or frequency domain. Therefore, in SM-TDM/FDM systems we have $\rho_{\mathrm{ml}}^{\mathrm{TF}} = \rho_{\mathrm{ml}}^{\mathrm{TF}} = P_{\mathrm{u}}$, where $\rho_{\mathrm{ml}}^{\mathrm{TF}}$ and $\rho_{\mathrm{fl}}^{\mathrm{TF}}$ represent the transmit power of ML and FL in SM-TDM/FDM systems, respectively. Then following from a same analysis of Section III A, the SE of ML and FL in SM-TDM/FDM systems can be lower bounded as (35) and (36), where $S_{\mathrm{ml}}^{\mathrm{TF}}$ and $S_{\mathrm{fl}}^{\mathrm{TF}}$ denote the SE lower bound of ML and FL in SM-TDM/FDM systems, respectively. The SINR of the n-th TA for ML and the SINR of the m-th TA for FL in SM-TDM/FDM systems are denoted as $\mathrm{SINR}_{\mathrm{ml},n}^{\mathrm{TF}}$ and $\mathrm{SINR}_{\mathrm{fl},m}^{\mathrm{TF}}$, respectively. With respect to L_{ml}

and L_{fl}, for SM-TDM systems, $L_{\mathrm{ml}} + L_{\mathrm{fl}}$ denotes the total time duration, and L_{ml} and L_{fl} are transmission time for ML and FL, respectively. For SM-FDM systems, $L_{\mathrm{ml}} + L_{\mathrm{fl}}$ represent the total bandwidth, and L_{ml} and L_{fl} are bandwidth for ML and FL, respectively. In addition, $\mathbf{\Sigma}_{\mathrm{ml},n}^{\mathrm{TF}}$ can be denoted as follows:

$$
\mathbf{\Sigma}_{\mathrm{ml},n}^{\mathrm{TF}} = \mathrm{diag}\left\{ \frac{1}{\mathrm{SINR}_{\mathrm{ml},1}^{\mathrm{TF}}}, ..., \frac{1}{\mathrm{SINR}_{\mathrm{ml},N_{\mathrm{t}}}^{\mathrm{TF}}} \right\} + N_{\mathrm{t}}\mathrm{diag}\{\hat{\mathbf{a}}_{\mathrm{ml},n}\},
\tag{37}
$$

and $\mathbf{\Sigma}_{\mathrm{fl},m}^{\mathrm{TF}}$ can be denoted as follows:

$$
\mathbf{\Sigma}_{\mathrm{fl},m}^{\mathrm{TF}} = \mathrm{diag}\left\{ \frac{1}{\mathrm{SINR}_{\mathrm{fl},1}^{\mathrm{TF}}}, ..., \frac{1}{\mathrm{SINR}_{\mathrm{fl},N_{\mathrm{t}}}^{\mathrm{TF}}} \right\} + N_{\mathrm{t}}\mathrm{diag}\{\hat{\mathbf{a}}_{\mathrm{fl},m}\}.
\tag{38}
$$

Since ML services and FL services are transmitted separately in SM-TDM/FDM systems, only ML transmit symbols constitute the IAI of the $\mathrm{SINR}_{\mathrm{ml},n}^{\mathrm{TF}}$, and only FL transmit symbols constitute the IAI of the $\mathrm{SINR}_{\mathrm{fl},m}^{\mathrm{TF}}$. Besides, for both transmission of ML and FL, the transmit power need not to be split. Therefore, it can be easily derived as follows:

$$
\begin{aligned}
\mathrm{SINR}_{\mathrm{ml},n}^{\mathrm{TF}} &= \frac{P_{\mathrm{u}} N_{\mathrm{rm}}}{N_{\mathrm{t}}(P_{\mathrm{u}} + \sigma_{\mathrm{ml}}^2)}, \\
\mathrm{SINR}_{\mathrm{fl},m}^{\mathrm{TF}} &= \frac{P_{\mathrm{u}} N_{\mathrm{rf}}}{N_{\mathrm{t}}(P_{\mathrm{u}} + \sigma_{\mathrm{fl}}^2)},
\end{aligned}
\tag{39}
$$

and thus the closed-form SE lower bound for both ML and FL in SM-TDM/FDM systems can also be formulated.

V. SIMULATION RESULTS

In this section, Monte Carlo simulations are provided to verify the tightness of the SE lower bound for SM-LDM systems, and the SE comparison between SM-LDM systems, single-TA LDM systems and SMX-LDM systems is also illustrated via simulations. Besides, it should be pointed out that we set SNR rather than SINR as the as the x-coordinate in Figures 3-5. This is because the SINR is an intermediate variable depending on the number of TAs, the number of RAs and SNR. Thus using the independent variable SNR as the x-coordinate is more reasonable.

A. Bound Tightness

In this subsection, the tightness of our proposed SE lower bound for SM-LDM systems is verified. In Fig. 2 (a), $N_{\mathrm{t}} = 2$, $N_{\mathrm{rf}} = 2$, $N_{\mathrm{rm}} \in \{1, 2, 4, 8\}$, $IL \in \{5 \text{ dB}, 20 \text{ dB}\}$ and $\mathrm{SNR}_{\mathrm{ml}} = 0$ dB are assumed, where $\mathrm{SNR}_{\mathrm{ml}}$ denotes the SNR of ML. In Fig. 2 (b), we assume $N_{\mathrm{t}} = 2$, $N_{\mathrm{rm}} = 2$, $N_{\mathrm{rf}} \in \{1, 2, 4, 8\}$, $IL \in \{5 \text{ dB}, 20 \text{ dB}\}$ and $\mathrm{SNR}_{\mathrm{fl}} = 20$ dB, where $\mathrm{SNR}_{\mathrm{fl}}$ denotes the SNR of FL. As shown in Fig. 2, our proposed SE lower bound is relatively tight. Comparing with (8) and (9), it can be observed that the gap between the theoretical SE and SE lower bound is from the approximation of spatial-domain MI. In addition, because of the RA diversity, increasing N_{rm} and N_{rf} can increase the SE of ML and FL, respectively. However, for both ML and FL, a larger number of RAs brings a larger gap between our proposed SE lower bound and theoretical SE. This is because more RAs brings a larger spatial-domain MI, and the proportion between the lower bound and theoretical value

$$S_{\text{ml}}^{\text{TF}} = \frac{L_{\text{ml}}}{L_{\text{ml}} + L_{\text{fl}}} \left\{ \log_2(N_{\text{t}}) - N_{\text{t}} + \frac{1}{N_{\text{t}}} \left[\sum_{n=1}^{N_{\text{t}}} \log_2 \left(1 + N_{\text{t}} \text{SINR}_{\text{ml},n}^{\text{TF}} \right) - \sum_{n=1}^{N_{\text{t}}} \log_2 \left(\sum_{n'=1}^{N_{\text{t}}} \frac{\det \left(\boldsymbol{\Sigma}_{\text{ml},n}^{\text{TF}} \right)}{\det \left(\boldsymbol{\Sigma}_{\text{ml},n}^{\text{TF}} + \boldsymbol{\Sigma}_{\text{ml},n'}^{\text{TF}} \right)} \right) \right] \right\}, \quad (35)$$

$$S_{\text{fl}}^{\text{TF}} = \frac{L_{\text{fl}}}{L_{\text{ml}} + L_{\text{fl}}} \left\{ \log_2(N_{\text{t}}) - N_{\text{t}} + \frac{1}{N_{\text{t}}} \left[\sum_{m=1}^{N_{\text{t}}} \log_2 \left(1 + N_{\text{t}} \text{SINR}_{\text{fl},m}^{\text{TF}} \right) - \sum_{m=1}^{N_{\text{t}}} \log_2 \left(\sum_{m'=1}^{N_{\text{t}}} \frac{\det \left(\boldsymbol{\Sigma}_{\text{fl},m}^{\text{TF}} \right)}{\det \left(\boldsymbol{\Sigma}_{\text{fl},m}^{\text{TF}} + \boldsymbol{\Sigma}_{\text{fl},m'}^{\text{TF}} \right)} \right) \right] \right\}, \quad (36)$$
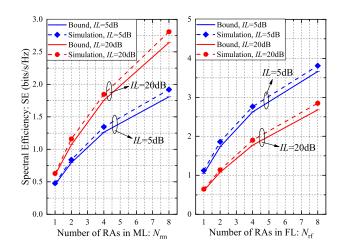

Fig. 2. The SE performance of simulation results and our proposed SE lower bound versus N_{rm} for ML in (a). The SE performance of simulation results and our proposed SE lower bound versus N_{rf} for FL in (b).
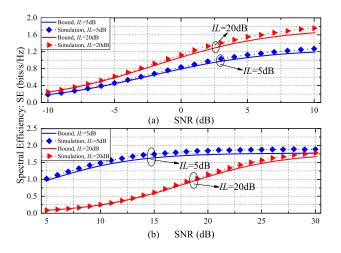

Fig. 3. The SE performance versus SNR based on simulation results and our proposed SE lower bound for ML in (a) and for FL in (b).

Fig. 4. The SE performance of ML in SM-LDM, single-TA LDM and SMX-LDM systems versus SNR with $N_{\text{rm}} = 2$, $N_{\text{rf}} = 2$ and $IL \in \{5 \text{ dB}, 20 \text{ dB}\}$. $N_{\text{t}} = 2$ in (a) and $N_{\text{t}} = 4$ in (b).

addition, from both Fig. 2 and Fig. 3, it can be illustrated that a larger IL brings a higher SE of ML, and a lower SE of FL.

In a word, our proposed SE lower bound of SM-LDM systems is relatively tight, and the bound and theoretical results is the same trend. Therefore, this SE lower bound will be utilized for the SE comparison in the next subsection.

B. SE Comparison

In this subsection, the SE comparison between different schemes are proposed via simulations. It should be pointed out that, N_{t} denotes the number of TAs in SM-LDM systems and SMX-LDM systems, but for single-TA LDM systems, we have $N_{\text{t}} = 1$. In addition, although in practice for Digital Terrestrial Television (DTT) the number of TAs in MIMO is 2 [9]–[11], recently the MIMO systems with more than 2 TAs [12]–[14], even massive MIMO systems have also been considered in broadcasting transmission scenarios [16] [17]. Therefore, in this subsection, we set $N_{\text{t}} \in \{1, 2, 4\}$. Comparing with traditional single-TA LDM system, our proposed SM-LDM system is equipped with more TAs and one more RF chain. Since the cost of TAs is much less than that of RF chains, the rising cost of the SM-LDM system is rather limited. In the SMX-LDM system, the number of RF chains is equal to the number of TAs, so the SM-LDM system has a lower cost than that of the SMX-LDM system.

From Fig. 4, it can be observed that the SM-LDM system always has a higher ML SE than that of the single-TA LDM system in a not so low SNR, which is because the spatial domain transmits extra information. Additionally, our proposed

almost remains unchanged. As the growing of RAs, although the gap between SE lower bound and theoretical SE becomes slightly bigger, the SE lower bound and theoretical SE result also have the same slope.

In Fig. 3, the system configurations include $N_{\text{t}} = 2$, $N_{\text{rm}} = 2$, $N_{\text{rf}} = 2$ and $IL \in \{5 \text{ dB}, 20 \text{ dB}\}$. From Fig. 3 (a), it can be observed that a larger SNR_{ml} leads to a higher SE in ML. From Fig. 3 (b), although a larger SNR_{fl} can also bring a higher SE in FL, when SNR_{fl} becomes relatively high, the SE of FL becomes almost saturated. This is because with quite high SNR, the IAI mainly brings influence on this interference-limited system, and MRC cannot eliminate the IAI in FL. In
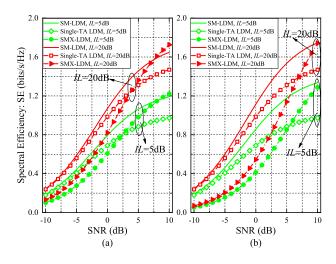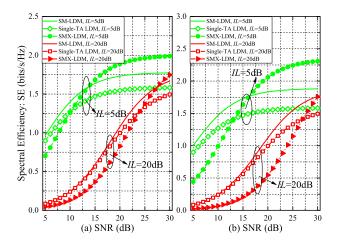
Fig. 5. The SE performance of FL in SM-LDM, single-TA LDM and SMX-LDM systems versus SNR with $N_{rm} = 2$, $N_{rf} = 2$ and $IL \in \{5 \text{ dB}, 20 \text{ dB}\}$. $N_t = 2$ in (a) and $N_t = 4$ in (b).

Fig. 6. The SE performance of ML and FL in SM-LDM and SM-TDM/FDM systems with $N_t \in \{1, 2, 4\}$, $N_{rm} = 2$, $N_{rf} = 2$, $SNR_{ml} = 0$ dB and $SNR_{fl} = 20$ dB.

SM-LDM system even has a better ML SE performance than that of the SMX-LDM system in a not so high SNR region. This is because the SNR for ML transmission is relatively low, and for fairness the transmit power of each TA in SMX-LDM system divides N_t comparing with SM-LDM system. Therefore, in this case, the AWGN mainly brings influence on this power-limited system, and the SMX-LDM system has a much lower SINR than that of the SM-LDM system. So SM-LDM system can outperform the SE of SMX-LDM system in a not so high SNR. As shown in Fig. 4 (a), in a high SNR_{ml}, the SE of the SMX-LDM system with $IL = 20$ dB is bigger than that of the SM-LDM system with $IL = 20$ dB. This is because with a high SNR and a big IL, the $SINR_{ml}$ of the SMX-LDM system is almost the same as the $SINR_{ml}$ of the SM-LDM system, and in this case the multiple constellation-domain symbols in SMX-LDM system transmit more information than the single constellation-domain symbol in SM-LDM system. In addition, from Fig. 4 (a) and Fig. 4 (b), it can be illustrated that increasing N_t can also increase the ML SE in SM-LDM systems, which is because a larger N_t brings a higher spatial-domain MI. However, for SMX-LDM systems, the SE with $N_t = 4$ is smaller than the SE with $N_t = 2$ when SNR is low. This is because for fairness, the transmit power of each TA in SMX-LDM systems divides N_t. From (34) and (31), it can be seen that comparing with SM-LDM systems, the SE of SMX-LDM systems is much influenced by growing of N_t in low SNR region. Besides, it can be shown from Fig. 4 that in a low SNR, the ML SE of SM-LDM system is almost the same as that of single-TA LDM system, which means that ML with low SNR need no multiple TAs. Our proposed SM-LDM system is more suitable for the not so low SNR.

As shown in Fig. 5, the SM-LDM system still has a higher FL SE than that of the single-TA LDM system because of the spatial-domain information. However, as the SNR becomes larger in FL, the FL SE of the SMX-LDM system exceeds the FL SE of the SM-LDM system. In other words, the SMX-LDM system can have a larger SE than that of SM-LDM system in a high SNR. This is because with a relatively high SNR for FL transmission, the IAI rather than the AWGN
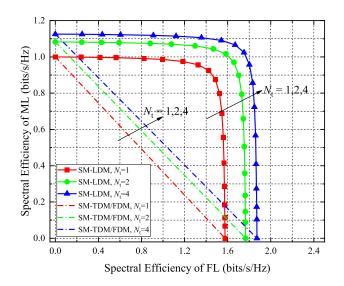
mostly influences the SINR. From (34) and (32), in FL, the IAI terms for both SM-LDM systems and SMX-LDM systems are similar, and in high SNR region, the AWGN terms for SM-LDM systems and SMX-LDM systems almost have the same influence on SINR. Therefore, with a high SNR in FL, the SINR of SM-LDM systems are almost the same as the SINR of SMX-LDM systems. In this case the constellation-domain MI in SMX-LDM systems is higher than the spatial-domain MI in SM-LDM systems, so with a high SNR the FL SE of SMX-LDM systems is higher than the FL SE of SM-LDM systems. Moreover, comparing to the system with $IL = 5$ dB, a larger SNR_{fl} is needed for the SMX-LDM system with $IL = 20$ dB exceeding the FL SE of SM-LDM system with $IL = 20$ dB, which is because a larger IL reduces the transmit power in FL. In addition, for SMX-LDM systems, in low SNR region, the FL SE with $N_t = 4$ is lower than that with $N_t = 2$, but in high SNR region, the FL SE with $N_t = 4$ is higher than that with $N_t = 2$. This is because in low SNR region, this system is a power-limited system, but in high SNR region, this system is an interference-limited system. In Fig. 5, the flattening curves for FL is caused by the IAI of FL, and this IAI cannot be eliminated by MRC. Since FL works in a high SNR region, the SE gain of the SM-LDM system over single-TA LDM system is fairly considerable, and the proposed SM-LDM system is pretty suitable in this case.

In Fig. 6, we compare the SE between SM-LDM systems and SM-TDM/FDM systems with different N_t. It can be observed that a larger N_t leads to a higher SE, but the SE gain between $N_t = 4$ and $N_t = 2$ is lower than that between $N_t = 2$ and $N_t = 1$. This is because although increasing N_t leads to a larger spatial-domain MI, a larger N_t also brings a larger IAI in (31) and (32). It can also be illustrated that the SM-LDM systems can outperform the SE of SM-TDM/FDM systems. In addition, for FL in SM-LDM systems, when IL is small enough, decreasing IL can hardly increase the FL SE, which is because in a small IL, it is a interference-limited system

for FL. Similarly, when *IL* is large enough, increasing *IL* can also barely increase the SE of ML. Besides, the maximum FL SE ranges from 1.6 bits/s/Hz to 2.0 bits/s/Hz, which is slightly low for broadcasting system operation. This is because the IAI cannot be cancelled by MRC, and employing the combining algorithms which can eliminate the IAI can enlarge the SE.

VI. CONCLUSION

In this paper, a SM-LDM system is proposed to increase the SE for terrestrial broadcasting transmission. The SE analysis framework is proposed with linear combining algorithms, and the closed-form SE lower bound for SM-LDM systems with MRC are also derived. In addition, for comparison, the closed-form SE of traditional single-TA LDM systems and SMX-LDM systems is also formulated. Our proposed SE analysis scheme can also be easily extended to the multi-layer SM-LDM systems. Simulation results are provided to validate the tightness of our proposed SE lower bound for SM-LDM systems, and SM-LDM systems can outperform the SE of SM-TDM/FDM systems and single-TA LDM systems. The SM-LDM systems can even have a higher SE than SMX-LDM systems in low SNR region via simulations.

REFERENCES

[1] L. Fay, L. Michael, D. Gómez-Barquero, N. Ammar, and M. W. Caldwell, "An overview of the ATSC 3.0 physical layer specification," *IEEE Trans. Broadcast.*, vol. 62, no. 1, pp. 233-243, Mar. 2016.

[2] T. Shitomi, E. Garro, K. Murayama, and D. Gómez-Barquero, "MIMO scattered pilot performance and optimization for ATSC 3.0," *IEEE Trans. Broadcast.*, to be published.

[3] S. I. Park, J. Y. Lee, S. Myoung, L. Zhang, Y. Wu, J. Montalbán, S. Kwon, B. M. Lim, P. Angueira, H. M. Kim, N. Hur, and J. Kim, "Low complexity layered division multiplexing system for ATSC 3.0," *IEEE Trans. Broadcast.*, vol. 62, no. 1, pp. 233-243, Mar. 2016.

[4] L. Zhang, W. Li, Y. Wu, X. Wang, S. I. Park, H. M. Kim, J. Y. Lee, P. Angueira, and J. Montalban, "Layered-division-multiplexing: Theory and practice," *IEEE Trans. Broadcast.*, vol. 62, no. 1, pp. 216-232, Mar. 2016.

[5] D. Gómez-Barquero and O. Simeone, "LDM vs. FDM/TDM for unequal error protection in terrestrial broadcasting systems: An information-theoretic view," *IEEE Trans. Broadcast.*, vol. 61, no. 4, pp. 571-579, Dec. 2015.

[6] L. Zhang, Y. Wu, W. Li, H. M. Kim, S. I. Park, P. Angueira, J. Montalban, and M. Velez, "Channel capacity distribution of layer-division-multiplexing system for next generation digital broadcasting transmission," in *Proc. IEEE BMSB*, pp. 1-6, Jun. 2014.

[7] R. Mesleh, H. Haas, S. Sinanovic, C. W. Ahn, and S. Yun, "Spatial modulation," *IEEE Trans. Veh. Technol.*, vol. 57, no. 4, pp. 2228-2241, Jul. 2008.

[8] M. Di Renzo, H. Haas, A. Ghrayeb, S. Sugiura, and L. Hanzo, "Spatial modulation for generalized MIMO: challenges, opportunities and implementation," *Proceedings of the IEEE*, vol. 102, no. 1, pp. 56-103, Jan. 2014.

[9] D. Vargas, D. Gozalvez, D. Gómez-Barquero, and N. Cardona, "MIMO for DVB-NGH, the next generation mobile TV broadcasting," *IEEE Trans. Broadcast.*, vol. 51, no. 7, pp. 130-137, Jul. 2013.

[10] D. Gómez-Barquero, D. Vargas, M. Fuentes, P. Klenner, S. Moon, J. Y. Choi, D. Schneider, and K. Murayama, "MIMO for ATSC 3.0," *IEEE Trans. Broadcast.*, vol. 62, no. 1, pp. 298-305, Mar. 2016.

[11] S. Saito, T. Shitomi, S. Asakura, A. Satou, M. Okano, K. Murayama, and K. Tsuchida, "8K terrestrial transmission field tests using dual-polarized MIMO and higher-order modulation OFDM," *IEEE Trans. Broadcast.*, vol. 62, no. 1, pp. 306-315, Mar. 2016.

[12] K. S. Woo, K. I. Lee, J. H. Paik, K. W. Park, W. Y. Yang, and Y. S. Cho, "A DSFBC-OFDM for a next generation broadcasting system with multiple antennas," *IEEE Trans. Broadcast.*, vol. 53, no. 2, pp. 539-546, Jun. 2007.

[13] I. Lee, S. Kim, H. Lee, B. Kwon, S. Lee, and K. Cho, "Optimal beam steering for maximal visual quality over a multimedia broadcasting system," *IEEE Trans. Broadcast.*, vol. 62, no. 1, pp. 35-45, Mar. 2016.

[14] D. Vargas, Y. J. D. Kim, J. Bajcsy, D. Gómez-Barquero, and N. Cardona, "A MIMO-channel-precoding scheme for next generation terrestrial broadcast TV systems," *IEEE Trans. Broadcast.*, vol. 61, no. 3, pp. 445-456, Sep. 2015.

[15] J. H. Seo, T. J. Jung, H. M. Kim, and D. S. Han, "Improved polarized 2x2 MIMO spatial multiplexing method for DVB-NGH system," *IEEE Trans. Broadcast.*, vol. 61, no. 4, pp. 729-733, Dec. 2015.

[16] H. Luo, Y. Zhang, L. K. Huang, J. Cosmas, and A. Aggoun, "A closed-loop reciprocity calibration method for massive MIMO in terrestrial broadcasting systems," *IEEE Trans. Broadcast.*, vol. 63, no. 1, pp. 11-19, Mar. 2017.

[17] B. Gong, L. Gui, Q. Qin, and X. Ren, "Compressive sensing-based detector design for SM-OFDM massive MIMO high speed train systems," *IEEE Trans. Broadcast.*, vol. 63, no. 4, pp. 714-726, Aug. 2017.

[18] T. Wang, S. Liu, F. Yang, J. Wang, J. Song, and Z. Han, "Generalized spatial modulation-based multi-user and signal detection scheme for terrestrial return channel With NOMA," *IEEE Trans. Broadcast.*, pp. 1-9, Oct. 2017.

[19] E. Garro, J. J. Gimenez, S. I. Park, and D. Gómez-Barquero, "Layered division multiplexing with multi-radio-frequency channel technologies," *IEEE Trans. Broadcast.*, vol. 62, no. 2, pp. 365-374, Jun. 2016.

[20] E. Björnson, E. G. Larsson, and M. Debbah, "Massive MIMO for maximal spectral efficiency: how many users and pilots should be allocated?" *IEEE Trans. Wireless Commun.*, vol. 15, no. 2, pp. 1293-1308, Feb. 2016.

[21] Y. Yang and B. Jiao, "Information-guided channel-hopping for high data rate wireless communication," *IEEE Commun. Lett.*, vol. 12, no. 4, pp. 225-227, Apr. 2008.

[22] A. M. Tulino and S. Verdú, "Random matrix theory and wireless communications," *Foundations Trends Commun. Inf. Theory*, vol. 1, no. 1, pp. 1-182, Jun. 2004.

Yue Sun (S'16) received the B.S. degree from the Department of Electronic Engineering in Tsinghua University, Beijing, China, in 2015. He is now pursuing the Ph.D. degree in the DTV Technology R&D Center, Department of Electronic Engineering in Tsinghua University. His research interests lie in the field of 5G wireless technologies, multiple-input multiple-output (MIMO) systems, and spatial modulation (SM) technique.

Jintao Wang (SM'12) received the B.Eng. and Ph.D. degrees in electrical engineering from Tsinghua University, Beijing, China, in 2001 and 2006, respectively. From 2006 to 2009, he was an Assistant Professor with the Department of Electronic Engineering, Tsinghua University. Since 2009, he has been an Associate Professor and a Ph.D. Supervisor. He has authored over 100 journal and conference papers and holds over 40 national invention patents. His current research interests include space-time coding, MIMO, and OFDM systems. He is a Standard Committee Member of the Chinese National Digital Terrestrial Television Broadcasting Standard.

Changyong Pan, born in Anhui province, China, in 1975, is a full professor in the Research Institute of Information Technology and deputy director of DTV R&D Center of Tsinghua University. Prof. Pan has authored or co-authored more than 180 technical papers and published 8 technical book. He holds 34 patents, won national technical award three times and is also the winner of numerous other awards.

Bo Ai (M'00-SM'10) received the Masters and Ph.D. degrees from Xidian University, Xian, China, in 2002 and 2004, respectively. He is currently working with Beijing Jiaotong University, Beijing, China, as a Professor and Advisor of Ph.D. candidates. He is also a Deputy Director of the State Key Laboratory of Rail Traffic Control and Safety. He is the author or coauthor of 8 books, 300 academic research papers, and 26 invention patents in his research area up to now. His interests include the research and applications of channel measurement and channel modeling, dedicated mobile communications for rail traffic systems.

Dr. Ai serves as an Editor of IEEE Transactions on Consumer Electronics and an Editorial Committee Member of the Wireless Personal Communications journal. He is the Lead Guest Editor for Special Issues on IEEE Transactions on Vehicular Technology, IEEE Antennas and Propagations Letters, International Journal on Antennas and Propagations. He received the Excellent Postdoctoral Research Fellow Award from Tsinghua University, Beijing, in 2007. He is a Fellow of the Institution of Engineering and Technology (IET Fellow).

Longzhuang He (S'15) received the bachelor's degree from the Department of Electronic Engineering at Tsinghua University, Beijing, China, in 2014. He is now pursuing the Ph.D. degree at the Department of Electronic Engineering in Tsinghua University. His research interests include multiple-input multiple-output (MIMO) systems, spatial modulation (SM) technique, and communication signal processing.